

MIMO Self-Heterodyne OFDM

Nirmal Fernando, Yi Hong *Senior Member, IEEE*, and Emanuele Viterbo *Fellow, IEEE*,

Abstract—Self-heterodyne OFDM (self-het OFDM) is a promising physical layer technique for millimeter-wave and terahertz RF communication due to its simple RF frontend and complete immunity against frequency-offset and phase noise. In this paper, we proposed a multiple-input multiple-output (MIMO) self-het OFDM with the adaptation of smart carrier position (SCP) technique. At the transmitter, a space-time block code (STBC) is used to produce the coded information symbols to be transmitted on each antenna over the self-het OFDM subcarriers. At the receiver, a simple non-linear detection is adopted at each receive antenna. The achievable diversity order of such setting is analysed, and it is found that with the adaptation of SCP technique, the diversity loss in comparison to the conventional coherent MIMO-OFDM can be compensated. We further derive analytically both lower and upper bounds on the diversity order of the proposed scheme and simulations will be shown to illustrate the performance of such combination.

Index Terms—Alamouti code, Golden code, MIMO, OFDM, self-heterodyne, non-coherent detection, direct detection, millimeter-wave, Terahertz RF.

I. INTRODUCTION

High speed indoor multimedia networking has driven a growing research interest in millimeter-wave and terahertz RF communications thanks to the availability of large chunks of free spectrum. However, coherent demodulation front-end components, such as carrier phase recovery phase lock loop circuits and oscillators, are complex and highly sensitive [1], [2]. In particular, these RF components generate high phase noise at the receiver and advanced frequency stabilization techniques are needed to control it at the expense of high receiver complexity [3].

An alternative approach is to use direct detection (DD) techniques, based on zero bias (ZB) Schottky barrier diodes [4] and micromachined millimeter-wave integrated circuits (MMIC) [5], [6]. These devices are equipped with near ideal “square law” characteristics, where the output electrical signal is directly proportional to the squared received RF signal magnitude. Moreover, these semiconductor devices have excellent phase noise performance and can replace complex frequency stabilization techniques at the receiver.

The self-heterodyne (self-het) down-conversion technique [3] together with the DD technique can provide simple and stable RF receivers for millimeter-wave and terahertz RF frequencies. Self-het down-conversion was originally proposed to combat phase noise in 60GHz RF bands. Later in [7], it

was shown experimentally that this technique can be used in conjunction with OFDM (i.e. self-het OFDM), where the sensitivity to phase noise is critical in choosing the subcarrier spacing. In self-het OFDM, the transmitter sends jointly the RF carrier and the OFDM subcarriers separated by a guard band. The insertion of the guard band reduces the bandwidth efficiency of self-het OFDM by 50% [18]. At the receiver, a self-mixing square-law device (e.g. ZB Schottky diode detector circuit) is used to down-convert the RF signal without the need of a local carrier, carrier phase recovery, and carrier frequency correction. The role of the guard band is to avoid self mixing interference produced by the nonlinear device. Since the transmitter can ensure the local carrier phase is synchronized with the OFDM subcarriers, the self-het OFDM down-conversion is simple, stable, and immune to phase noise. In [8], it was experimentally demonstrated that MMIC with multiple passive detectors can significantly increase the receiver sensitivity. Since then, there has been a number of recent research developments on self-het OFDM, as shown in [9], [10], [11], [12], [13].

Early study on channel characteristics of millimeter-wave RF channels suggests that these channels can be frequency selective in both line-of-sight (LOS) and non-LOS conditions [14], [15]. This is mainly due to the reflective nature of millimeter wave RF signals [16], [17]. In [18], we analyze self-het OFDM for a SISO frequency selective channel. A pairing scheme is then presented in [19] to exploit the unbalance in signal-to-interference plus noise ratios (SINRs) naturally occurring in the subcarriers of a self-het OFDM.

In this paper, we extend our previous study on SISO self-het OFDM [18] to a MIMO setting. For MIMO millimeter-wave communications, it was suggested in [20], [21] that directional antennas are needed to compensate for the path loss and enhance receive power for such small wavelengths. Such a setting results in a sparse multipath channel. It was also pointed out in [20], [21] that it is possible to obtain a high rank MIMO channel by using multiple antennas spaced several wavelengths apart. On one hand, to combat multipath effect, conventional OFDM techniques can be used, where each subcarrier is assumed to experience an independent fading that can be modeled as i.i.d. complex Gaussian random variables. On the other hand, better performance of MIMO millimeter-wave communications can be obtained by using space-time coding technique, as demonstrated in [20]. In this paper, we consider a space-time block coded (STBC) MIMO self-het OFDM¹ to achieve good performance by mitigating multipath effects and high-levels oscillator instabilities with an extremely low complexity RF front end. The specific contributions of our

¹This is also known as space-frequency block coded MIMO, which is performed across OFDM tones to obtain MIMO space and frequency diversity [22].

paper are:

- We consider the well-known Alamouti code [23] and the Golden code [25], respectively, as the STBC schemes. As an approximate measure of quality, we analyze the diversity order of STBC MIMO self-het OFDM and find there is a diversity loss, when compared to the traditional STBC MIMO-OFDM. This is due to the use of a common RF carrier from each transmit antenna in MIMO self-het OFDM. Specifically, the STBC MIMO self-het OFDM experiences a doubly faded channel, where one fade is due to multipath and the other is incurred by the RF carrier in each link between TX/RX antenna pairs.
- To compensate this loss, we modify the *smart carrier positioning* (SCP) technique, originally proposed in [18] for the SISO case. In the SISO case, the carrier was positioned in an OFDM subchannel with the highest gain to improve the bit error rate (BER) of the system. In the MIMO case, a common carrier is placed in a subcarrier position that jointly maximizes the overall MIMO channel gain and optimizes the diversity order. Under such a setting, we analyze the achievable diversity gain of the proposed SCP scheme. We first derive both upper and lower bounds on the diversity gain. We then show analytically and by simulation that the SCP STBC MIMO self-het OFDM can increase the diversity gain.

The paper is organized as follows. In Section II, we introduce the system model for MIMO self-het OFDM. In Section III, we consider two STBCs (Alamouti code and the Golden code) for MIMO self-het OFDM and we prove there is a diversity loss in such a system. In Section III, we present the SCP technique to compensate this diversity loss and we prove theoretically that SCP can improve diversity order by at least one. In Section V, we show the simulation results. Finally, we draw the conclusions in Section VI.

Throughout this paper, we adopt the following notation: $\Re\{\cdot\}$ denotes the real component of a complex number, j denotes the imaginary unit, $*$ represents the convolution operation, $|a|$ represents the absolute value of a , A^H represents the Hermitian matrix of A , $\mathbb{C}^{M \times N}$ represents an $M \times N$ complex matrix, $E[x]$ represents the expectation of a random variable x , $f_X(x)$ denotes the probability distribution function of random variable X , $\mathcal{L}(x)$ represents the Laplace transform of x , $K_v(\cdot)$ denotes the v -th order of modified Bessel function of second kind, $\mathbb{Ei}(x)$ is the exponential integral and defined by

$$\mathbb{Ei}(z) \triangleq - \int_z^\infty \exp(-t)/t dt,$$

and $Q(x)$ is the Gaussian tail function, defined by

$$Q(x) \triangleq \frac{1}{\sqrt{2\pi}} \int_x^\infty \exp(-u^2/2) du$$

II. SYSTEM MODEL

A. MIMO Self-het OFDM

A block diagram of a typical MIMO self-het OFDM communications system is shown in Fig. 1, where \mathbf{H} is the MIMO

channel frequency responses matrix, N_t is the number of transmit antennas, N_r is the number of receive antennas, f_c is RF carrier frequency, Δf is OFDM subcarrier spacing, N_s is the number of OFDM subcarriers used to encode information at each transmit antenna, N_g is the number of subcarriers omitted in each self-het OFDM transmitter, N ($N = N_g + N_s$) is the size of IFFT/FFT, B_g is the frequency gap between the RF carrier and the first OFDM subcarrier, and B_s is the useful OFDM subcarrier bandwidth.

At the transmitter, the information is encoded by a space-time encoder to generate the codeword matrix. Let $\mathbf{X}[k] \triangleq \{X_{mn}[k]\} \in \mathbb{C}^{N_t \times T}$ be the codeword matrix transmitted using N_t transmit antennas in the k -th OFDM subcarrier over T channel uses, where $m = 1, \dots, N_t$, $n = 1, \dots, T$, and $k = 1, \dots, N_s$. This coded symbol matrix is then fed column by column into N_t parallel self-het OFDM transmitters that use only the last N_s OFDM subcarriers for the transmission, while the remaining N_g OFDM subcarriers are set to zero (see Fig. 1). In each self-het OFDM transmitter by using an IFFT, the discrete time-domain OFDM symbol is generated as

$$s_m^{(n)}(t) = \Re \left\{ \sum_{k=1}^{N_s} X_{mn}[k] e^{j2\pi(B_g + k\Delta f)t} \right\} \quad (1)$$

where $B_g = N_g \Delta f$. The parallel-to-serial (PS) conversion, the addition of cyclic prefix (CP), and the digital-to-analog (DA) conversion are performed to generate the continuous time-domain OFDM symbol. Then, the RF signal $x_m^{(n)}(t)$ is generated by adding a RF carrier signal to $s_m^{(n)}(t)$ with a frequency gap B_g between the carrier and the first OFDM subcarrier², i.e.,

$$x_m^{(n)}(t) = [A + s_m^{(n)}(t)] \cos(2\pi f_c t). \quad (2)$$

The up-converted OFDM symbols $x_m^{(n)}(t)$ are then transmitted over a MIMO channel using N_t transmit antennas. Let $w_r^{(n)}(t)$, $h_{rm}^{(n)}(t)$, $z_r^{(n)}(t)$ be the received signal at the r -th receive antenna ($r = 1, \dots, N_r$), the channel impulse response from the m -th transmitter to the r -th receive antenna and the noise component at the r -th receive antenna, respectively. Then $w_r^{(n)}(t)$ can be written as

$$w_r^{(n)}(t) = h_{rm}^{(n)}(t) * x_m^{(n)}(t) + z_r^{(n)}(t). \quad (3)$$

We assume the zero-mean white Gaussian noise $z_r^{(n)}(t)$ with variance σ^2 is added before the non-linear down-conversion, and it is AWGN, i.e., $(z_r^{(n)}(t) \sim \mathcal{N}(0, \sigma^2))$, where σ^2 denotes the noise power.

At the receiver, signal detection is performed using a non-linear devices at each receiver producing the output $|w_r^{(n)}(t)|^2$, in order to down-convert the passband signal to the baseband signal. Since the local carrier signal is embedded in the received signal, the above down-conversion does not require any local carrier generation, carrier phase recovery, and carrier frequency correction [18]. This down-conversion is more stable and simpler than that of conventional super-heterodyne down-conversion [3]. The down-converted signals are then

²This can equivalently be realized by inserting in the first OFDM subcarrier, a DC component A , as shown in Fig. 1.

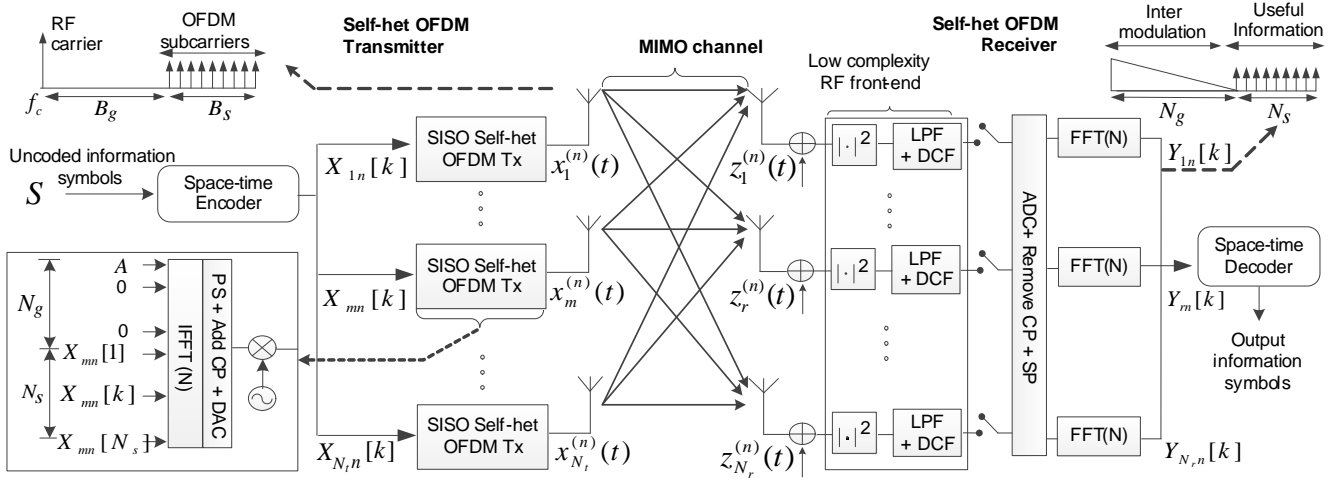


Fig. 1. MIMO self-Het OFDM.

passed through low pass filters (LPF), with a cutoff frequency $B_g + B_s$, and DC filters (DCF) to remove the high frequency signals and the residual DC components generated during the non-linear down-conversion. After the analog-to-digital conversion (ADC), the CP is removed, serial-to-parallel (SP) conversion is performed, and FFT recovers the transmitted symbols. As shown in [18], the condition $B_g \geq B_s$ is required in order to restrict the dominant inter-modulation product, generated by the non-linear down-conversion, occurring in the first N_g OFDM subcarriers. Hence, the first N_g OFDM subcarriers are ignored, since they contain only the intermodulation products, as shown in Fig. 1. The next N_s OFDM subcarriers that contain the transmitted symbols are forwarded to the space-time decoder to extract the transmitted information.

The discrete equivalent baseband model for a SISO channel, given in [18], can be extended to the MIMO case. For simplicity, in the following, we drop the index k , since we only consider one OFDM subcarrier at a time. For an arbitrary OFDM subcarrier, we have

$$\mathbf{Y} = \mathbf{H}_c^* \mathbf{H} \mathbf{X} + \hat{\mathbf{Z}} \quad (4)$$

where $\mathbf{Y} \triangleq \{Y_{rn}\} \in \mathbb{C}^{N_r \times T}$, $\mathbf{H} \triangleq \{H_{rm}\} \in \mathbb{C}^{N_r \times N_t}$, $\hat{\mathbf{Z}} \triangleq \{\hat{Z}_{rn}\} \in \mathbb{C}^{N_r \times T}$ represent the received symbol matrix, the frequency response of the MIMO channel, and the equivalent noise/interference component after the non-linear down-conversion, respectively. In (4), the diagonal matrix $\mathbf{H}_c \triangleq \text{diag}\{\sum_{m=1}^{N_t} H_{rm}^{(c)}\}$ with $H_{rm}^{(c)}$ represents the channel frequency response evaluated at the carrier frequency from the m -th transmit antenna to the r -th receive antenna. In moderate and high SNR regions, from equation (17) in Section III-B of [18], the noise variance for the subcarrier k at receiver r averaged over the channel realization \mathbf{H} , but conditioned on the carrier frequency response \mathbf{H}_c , is approximately given by

$$\sigma_{\hat{Z}_r}^2 \cong \sigma^2 \left(\left| \sum_{r=1}^{N_r} H_{rm}^{(c)} \right|^2 + \frac{\lambda_r(k)}{\eta N_s} \right) \quad (5)$$

where η denotes the RF carrier-to-signal power ratio [18], $k =$

$1, \dots, N_s$, $r = 1, \dots, N_r$, and

$$\lambda_r(k) \cong \sigma^2 \frac{2(N_s - k)}{(N_g + N_s)} \mathbf{E} \left[\sum_{k=1}^{N_s} \sum_{m=1}^{N_t} |H_{rm}^{(k)}|^2 \right] \quad (6)$$

Since

$$\mathbf{E} \left[\sum_{k=1}^{N_s} \sum_{m=1}^{N_t} |H_{rm}^{(k)}|^2 \right] = N_s N_t \quad (7)$$

and we assume $N_g = N_s$, we have

$$\sigma_{\hat{Z}_r}^2 = \sigma^2 \left(\left| \sum_{r=1}^{N_r} H_{rm}^{(c)} \right|^2 + \frac{N_t}{\eta N_s} (N_s - k) \right) \quad (8)$$

This shows that every subcarrier has a different signal-to-noise plus interference ratio (SINR).

III. STBC MIMO SELF-HET OFDM

In this Section, we will consider two types of space-time block codes for 2×2 MIMO self-het OFDM: (i) Alamouti code [23], and (ii) the Golden code [25]. For simplicity, we still drop the OFDM subcarrier index $k = 1, \dots, N_s$. It was pointed out in [20], [21], that by using multiple directional antennas spaced several wavelengths apart, the MIMO channels can be assumed to be independent. Since the multipath component channels can be equalised by the OFDM technique, we assume that the channel response coefficients for each subcarrier are i.i.d. complex Gaussian with zero mean and unit variance (also known as Rayleigh fading), i.e., $H_{rm}^{(c)}, H_{rm} \sim \mathcal{N}(0, 1)$, where $r = 1, 2$, and $m = 1, 2$.

A. Alamouti code [23]

Let $\mathbf{S} = [S_1, S_2]^T$ be the uncoded M -QAM information symbol vector to be transmitted over two consecutive OFDM symbols in the k -th OFDM subcarrier and the energy of each symbol is denoted by E_s . The Alamouti encoder generates the following codeword matrix [23]:

$$\mathbf{X} = \begin{bmatrix} S_1 & -S_2^* \\ S_2 & S_1^* \end{bmatrix}. \quad (9)$$

Let $\alpha_c \triangleq H_{11}^{(c)} + H_{12}^{(c)}$ and $\beta_c \triangleq H_{21}^{(c)} + H_{22}^{(c)}$. Using Alamouti pre-processing [23] and from (4), we have

$$\underbrace{\begin{bmatrix} Y_{11} \\ Y_{21} \\ Y_{12}^* \\ Y_{22}^* \end{bmatrix}}_{\triangleq \hat{\mathbf{Y}}} = \underbrace{\begin{bmatrix} \alpha_c^* H_{11} & \alpha_c^* H_{12} \\ \beta_c^* H_{21} & \beta_c^* H_{22} \\ \alpha_c H_{12}^* & -\alpha_c H_{11}^* \\ \beta_c H_{22}^* & -\beta_c H_{21}^* \end{bmatrix}}_{\triangleq \mathbf{H}_{\text{eq}}} \begin{bmatrix} S_1 \\ S_2 \end{bmatrix} + \underbrace{\begin{bmatrix} \hat{Z}_{11} \\ \hat{Z}_{21} \\ \hat{Z}_{12}^* \\ \hat{Z}_{22}^* \end{bmatrix}}_{\triangleq \hat{\mathbf{Z}}} \quad (10)$$

Let $\mathbf{H}_{\text{eq}}^\dagger$ be the pseudo-inverse of \mathbf{H}_{eq} , and

$$\begin{aligned} \mathbf{H}_{\text{eq}}^\dagger &\triangleq (\mathbf{H}_{\text{eq}} \mathbf{H}_{\text{eq}}^H)^{-1} \mathbf{H}_{\text{eq}}^H \\ &= \frac{1}{\Lambda} \mathbf{H}_{\text{eq}}^H \end{aligned} \quad (11)$$

where

$$\Lambda \triangleq \underbrace{|\alpha_c|^2 \left(\sum_{m=1}^2 |H_{1m}|^2 \right)}_{\triangleq \Lambda_1} + \underbrace{|\beta_c|^2 \left(\sum_{m=1}^2 |H_{2m}|^2 \right)}_{\triangleq \Lambda_2}. \quad (12)$$

At the receiver, zero forcing (ZF) equalizer or maximum likelihood detection (MLD) can be used to recover the information symbols by considering the $\mathbf{H}_{\text{eq}}^\dagger \hat{\mathbf{Y}}$ vector.

It is known that conventional MIMO-OFDM schemes using Alamouti code achieves diversity order of 4 in 2×2 MIMO systems [24]. However, in the following, we prove that MIMO self-het OFDM using Alamouti code only provides diversity 2.

Proposition 1: The achievable diversity order of 2×2 Alamouti coded MIMO self-het OFDM is 2 for MIMO channels.

Proof: See Appendix A. ■

We note that this diversity loss is due to the fact that the use of RF carrier undergoes independent fading from the same OFDM subchannel of the two incoming links at each receive antenna. Specifically, we can observe that the channel matrix in (10) is different from that of conventional Alamouti coded MIMO-OFDM schemes, where $\alpha_c = 1$ and $\beta_c = 1$. From (12) we observe that the carrier fading terms multiply the standard MIMO channel fading terms, resulting in a doubly faded channel, as we will analyze in the following section.

B. The Golden code [25]

The Golden code is an optimal full-rate full-diversity STBC code for a coherent 2×2 MIMO channel, which has non-vanishing determinant property [25] and achieves the diversity-multiplexing frontier [26]. Let $\mathbf{S} = [S_1, S_2, S_3, S_4]^T$ be the uncoded M -QAM information symbol vector to be transmitted over two consecutive OFDM symbols in the k -th OFDM subcarrier. The algebraic construction yields codewords of the Golden code of the form [25]

$$\mathbf{X} = \frac{1}{5} \begin{bmatrix} \alpha(S_1 + \theta S_2) & \alpha(S_3 + \theta S_4) \\ j\sigma(\alpha)(S_3 + \sigma(\theta)S_4) & \sigma(\alpha)(S_1 + \sigma(\theta)S_2) \end{bmatrix} \quad (13)$$

where $\theta = (1 + \sqrt{5})/2$, $\sigma(\theta) = 1 - \theta$, $\alpha = 1 + j\sigma(\theta)$ and $\sigma(\alpha) = 1 + j\theta$. Let \mathbf{G} be the generator matrix for the Golden code, i.e. $\mathbf{X} = \mathbf{G}\mathbf{S}$, and the \mathbf{G} matrix is given in [25]. At the

receiver, MLD is performed to decode the original information symbols as

$$\hat{\mathbf{S}} = \arg \min_S \|\mathbf{Y} - \mathbf{H}_c^* \mathbf{H} \mathbf{G} \mathbf{S}\|^2 \quad (14)$$

where $\hat{\mathbf{S}}$ is the estimated received symbol vector in the k -th OFDM subcarrier. Since the complexity of MLD grows exponentially with higher order signal constellations, sphere-decoder based MLD [27] can be used to achieve the best performance with reduced decoding complexity.

We remark that fast decodable STBC codes, e.g. silver code [29], [30], can be also implemented in MIMO, similarly to the Golden code.

IV. SELF-HET MIMO ENHANCEMENTS

A. SCP technique

In *Proposition 1* we show that STBC encoded MIMO self-het OFDM cannot exploit the full diversity gain. More specifically, it was shown in Appendix A that the diversity order of a communication system is directly related to the instantaneous SINR (γ) distribution of the OFDM subcarriers. The distribution of γ is determined by the behavior around zero of the distribution of the random variable Λ defined in (12). Hence, the diversity order of Alamouti coded MIMO self-het OFDM systems can be improved by optimizing the distribution of Λ . We therefore consider the *smart carrier positioning* (SCP) technique, originally proposed in [18] for the SISO case. Different from the SISO case, where the carrier was positioned in an OFDM subchannel with the highest gain, in MIMO case, the carrier will be placed in a subcarrier that maximizes jointly the MIMO channel gain and optimizes the diversity order, which is a standard measure of the performance of STBC [23], [28], [30]. The details on the proposed SCP for MIMO self-het OFDM is given below.

At the transmitter, the SCP places the RF carrier in either the lower or the upper band with respect to the OFDM subcarriers (see Fig. 2(a) and Fig. 2(b)). If the RF carrier is placed in the higher band, the information subcarriers can be transmitted in the lower band, and the transmitted OFDM symbols are $X_{mn}^*[k]$, instead of $X_{mn}[k]$. After the non-linear detection both subcarrier placements give the same result.

Let P be the total number of possible carrier positions (equally spaced by Δf), where $l \in \{1, \dots, P/2, N - P/2 - 1, \dots, N\}$ is the RF carrier position. Let us define

$$\alpha_c^{(l)} \triangleq H_{11}^{(l)} + H_{12}^{(l)} \quad \text{and} \quad \beta_c^{(l)} \triangleq H_{21}^{(l)} + H_{22}^{(l)}, \quad (15)$$

where $H_{rm}^{(l)}$ is the channel frequency response from the m -th transmit antenna to the r -th receive antenna at the l -th potential RF carrier position. If the channel length is considerably larger than the OFDM symbol duration, for a given OFDM symbol transmission, we assume that H_{rm} for $r, m = 1, 2$ are independent random variables from $\alpha_c^{(l)}$ and $\beta_c^{(l)}$. Since $E[|H_{rm}|^2] = 1$, where $r, m = 1, 2$, the expectation of Λ over k can be approximated as

$$E[\Lambda] \approx 2 \left(|\alpha_c^{(l)}|^2 + |\beta_c^{(l)}|^2 \right)$$

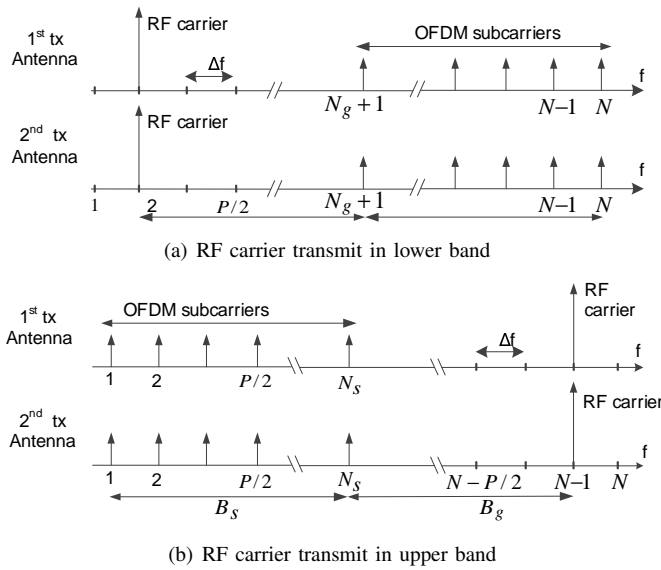


Fig. 2. SCP technique in STBC encoded MIMO self-het OFDM.

for a given l -th RF carrier position. As shown in Fig. 2, if the MIMO channel is known, we can select the optimum carrier position by

$$l^* = \arg \max_{\substack{l \in \{1, \dots, \frac{P}{2}, \\ N - \frac{P}{2}, \dots, N\}}} \left\{ \left(|\alpha_c^{(l)}|^2 + |\beta_c^{(l)}|^2 \right) \right\}, \quad (16)$$

where l^* denotes the optimum carrier position. For a general STBC MIMO-self-het OFDM, this optimization given in (16) can be extended as

$$l^* = \arg \max_{\substack{l \in \{1, \dots, \frac{P}{2}, \\ N - \frac{P}{2}, \dots, N\}}} \left\{ \sum_{r=1}^{N_r} \left| \sum_{m=1}^{N_t} H_{rm}^{(l)} \right|^2 \right\}. \quad (17)$$

After choosing the best l^* in (16), we let $p = l^*$, if the carrier is positioned on the left handside, or $p = N + 1 - l^*$, if on the right handside. Then we have $B_g = B_s = \Delta f(N + 1 - p)/2$, where $p \in \{1, 2, 3, \dots, P/2\}$. We will show in Section V that the SCP technique for the MIMO case requires very limited number of feedback information, i.e., a few information bits to encode the index l^* .

B. Diversity order of SCP STBC MIMO Self-Het OFDM

The diversity order of an STBC measures the reliability of the $N_t \times N_r$ MIMO communication system. We say the STBC has full diversity when the order is equal to $N_t \cdot N_r$. In this subsection, we analyze the diversity order of 2×2 Alamouti coded MIMO self-het OFDM using SCP ($P = 2$) over MIMO channels and we have the following propositions.

Proposition 2: The lower bound on the diversity order of 2×2 Alamouti coded MIMO self-het OFDM using SCP is 3.

Proof: see Appendix B. ■

Proposition 3: The upper bound on the diversity order of 2×2 Alamouti coded MIMO self-het OFDM using SCP is 4.

Proof: see Appendix C. ■

We conclude that the actual diversity order of MIMO self-het OFDM is between 3 and 4. Due to the doubly fading effects the order is not necessarily an integer value.

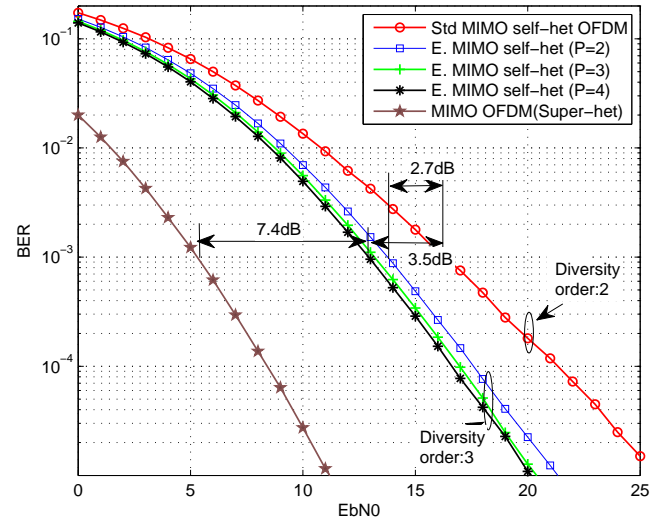


Fig. 3. BER performance of 2×2 MIMO self-het OFDM using the Alamouti code and SCP technique (no phase noise).

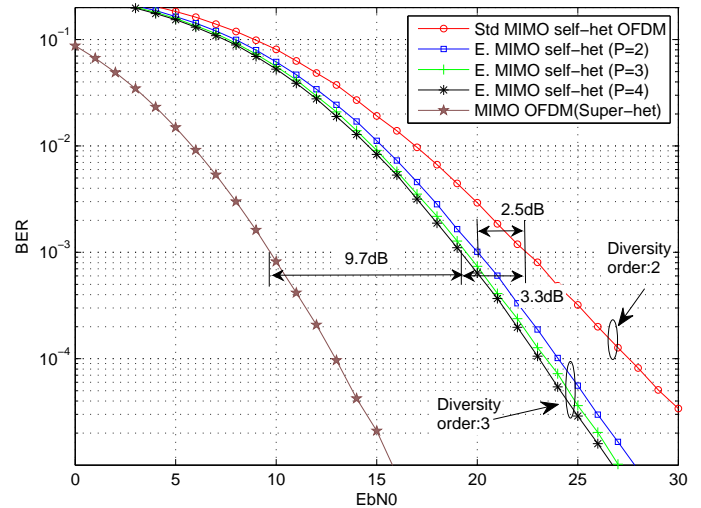


Fig. 4. BER performance of 2×2 MIMO self-het OFDM using the Golden code and SCP technique (no phase noise).

V. SIMULATION RESULTS

In this section, we simulate the BER performance of 2×2 MIMO self-het OFDM. We adopt the following simulation parameters: $N = 256$, $N_s = N_g = 128$, $\eta = 0.6$, sampling time $T_s = 1 \mu s$, the maximum channel delay $64 T_s$, the length of CP of $(64 + 1)T_s$, and QPSK signalling. With QPSK signalling, since half of OFDM subcarriers are unused in self-het OFDM, the spectral efficiency of self-het OFDM is 50% of that achieved by the conventional OFDM scheme using super-heterodyne structure. For comparison, we use BPSK signaling in conventional MIMO OFDM in order to have the same spectral efficiency.

Fig. 3 compares the BER performance of standard MIMO self-het OFDM and enhanced MIMO self-het OFDM using

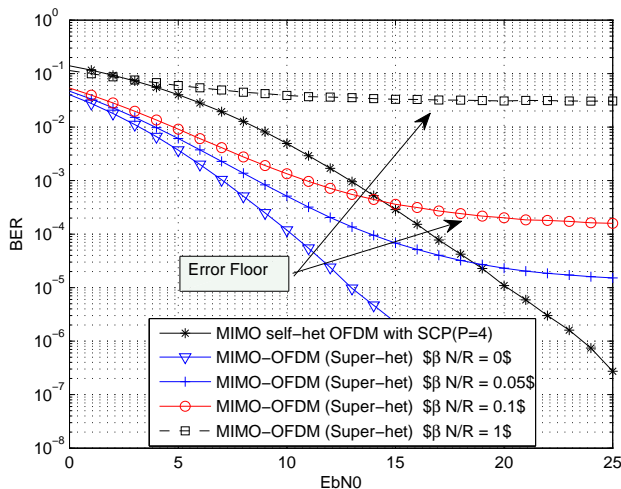


Fig. 5. BER performance comparison of Alamouti coded MIMO self-het OFDM with SCP ($P = 4$) and Alamouti coded MIMO-OFDM with super-heterodyne in the presence of phase noise ($R = 2.133 \times 10^7$).

SCP technique. Both of the systems are encoded with an Alamouti code. In this simulation, we assume no phase noise at the receiver. In contrast to standard MIMO self-het OFDM, the enhanced scheme provides approximately 2.7dB and 3.5dB gains at BER of 10^{-3} with $P = 2$ and $P = 4$, respectively. For $P \ll N$, the SCP technique consumes a negligible amount of extra bandwidth. We also observe that $P = 4$ is a good compromise, since the gain saturates for $P > 4$, and the rate loss at $P = 4$ is negligible. As shown in Proposition 1, the diversity order of standard Alamouti coded MIMO self-het OFDM is 2, which is half of that in a conventional Alamouti coded MIMO-OFDM. As discussed in Propositions 2 and 3, the diversity order of enhanced MIMO self-het OFDM using Alamouti code is between 3 and 4. In Fig. 3, the simulation results agrees with this analytical result. Furthermore, compared to Alamouti coded MIMO-OFDM with super-heterodyne structures, the enhanced Alamouti coded MIMO self-het OFDM has approximately 7.4dB performance loss at BER of 10^{-3} . The performance loss is due to the fact that approximately half of transmitted power is spent for the transmission of the RF carrier, as well as 50% rate loss required to enable the non-linear detection. Nevertheless, we remark that MIMO self-het OFDM has the advantage of using an extremely low complexity RF frontend as well as phase noise immunity, which is not available in conventional OFDM with super-heterodyne structures.

Fig. 4 compares the BER performance of a standard 2×2 MIMO self-het OFDM and the enhanced 2×2 MIMO self-het OFDM. In this simulation, we assume no phase noise at the receiver and both systems are encoded by the Golden code. We see the enhanced scheme provides 2.5dB and 3.3dB gains at BER of 10^{-3} for $P = 2$ and $P = 4$ compared to the standard one, respectively. A diversity gain similar to that of the Alamouti code (from 2 to 3) is observed when using the Golden code. We note that the coded enhanced scheme is approximately 9.7dB worse than MIMO-OFDM with super-

heterodyne structures at BER of 10^{-3} [18].

Fig. 5 compares the BER performance of Alamouti coded MIMO self-het OFDM with SCP ($P = 4$) and Alamouti coded MIMO-OFDM with super-heterodyne in the presence of phase noise. Here, we adopted the OFDM phase noise model used in [31] to simulate the phase noise at the receiver only. We ignore the phase noise generated at the transmitter, since it is comparatively insignificant compared to the receiver phase noise and common for both OFDMs. The level of oscillator instabilities is measured by the phase-noise linewidth β , and the simulation results are presented for $N\beta/R = 0$ (no phase noise), 0.05, and 0.1, where $R = 2.133 \times 10^7$ is the sampling rate. We see that, for example, when $N\beta/R = 0.1$, we have $\beta \approx 8\text{KHz}$. This demonstrates that, when the phase-noise linewidth β is about 0.8% of the OFDM subcarrier spacing $\Delta f = 1\text{MHz}$, the conventional OFDM with super-heterodyne structure experiences error floor due to the loss of orthogonality among the subcarriers. For 60GHz, it was pointed out in [32] that, assuming the same reference oscillator, 60GHz signals suffer from phase noise that is 10 times greater when compared to unlicensed wireless systems below 6GHz. This indicates that, for 60GHz, using the same OFDM system as the above, the phase-noise linewidth β is about 8% of the OFDM subcarrier spacing and the conventional OFDM experiences an even higher error floor, as illustrated in Fig. 5.

As shown in Fig. 5, for the Alamouti coded MIMO-OFDM with super-heterodyne receiver structures, an error floor occurs depending upon the level of oscillator instabilities at the receiver. Hence, our scheme using SCP outperforms the Alamouti coded MIMO-OFDM with super-heterodyne structures at high SNRs.

Similar behavior is observed for the Golden coded MIMO self-het OFDM (see Fig. 6). Compared to Alamouti code, the Golden code is more sensitive to the phase noise, and the error floor occurs at lower SNRs. Hence, Golden coded MIMO self-het OFDM outperforms the conventional MIMO-OFDM at practical SNRs ranges (e.g. at SNR = 15dB when $N\beta/R = 0.1$ and $N\beta/R = 0.1$).

Finally, we simulate our Alamouti and Golden coded self-het OFDM with SCP ($P=4$) and conventional MIMO-OFDM in Figs. 7 and 8, respectively, using the parameters from the IEEE 802.11ad standard [35][36][37]. In both figures, we adopt rate 1/2 LDPC as an outer code with parity check matrix given in [37], and phase noise model in [36], i.e., the phase noise linewidth relative to subcarrier spacing is 0.3 ($\beta N/R = 0.3$). We use $N = 512$, $N_s = N_g = 256$, 25% cyclic prefix, $T_s = 46\text{ns}$, and 50 iterations of LDPC decoding. We adopt QPSK and BPSK signalling for self-het OFDM and conventional OFDM, respectively, to guarantee the same spectral efficiency. We observe that, although the channel code lowers the error floor of the conventional OFDM, the self-het OFDM BER will cross over and will not present any flooring effect.

VI. CONCLUSIONS

In this paper, we considered Alamouti and Golden coded 2×2 MIMO self-het OFDM with a simple non-linear detection

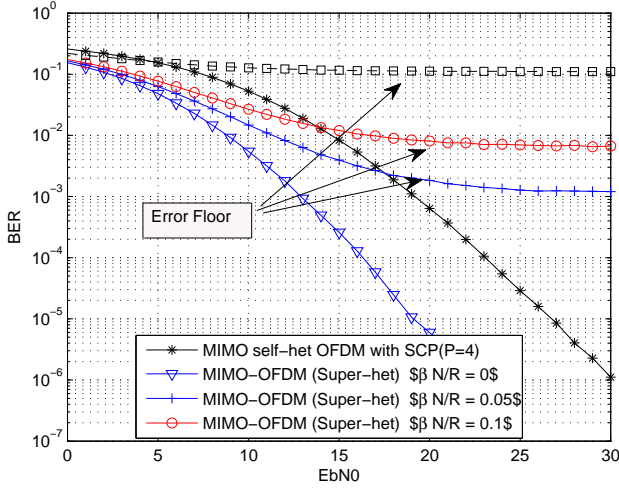


Fig. 6. BER performance comparison of Golden coded MIMO self-het OFDM with SCP ($P = 4$) and Golden coded MIMO-OFDM with superheterodyne in the presence of phase noise ($R = 2.133 \times 10^7$).

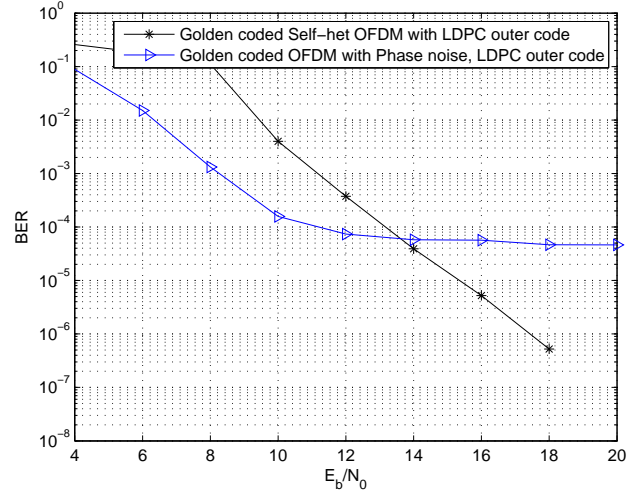


Fig. 8. BER performance comparison of Golden coded enhanced MIMO self-het OFDM with SCP ($P = 4$) and Golden coded MIMO-OFDM with common phase noise compensation, phase noise level ($\beta N/R = 0.3$), rate 1/2 LDPC as an outer code for both schemes.

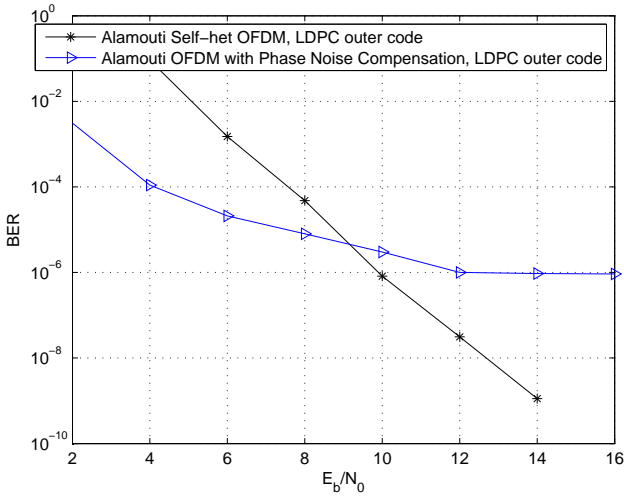


Fig. 7. BER performance comparison of Alamouti coded enhanced MIMO self-het OFDM with SCP ($P = 4$) and Alamouti coded MIMO-OFDM with common phase noise compensation, phase noise level ($\beta N/R = 0.3$), rate 1/2 LDPC as an outer code for both schemes.

at the receive antennas. For Alamouti code, we analytically proved that there is a diversity loss, which can be compensated by the proposed SCP technique. We then showed, by simulations, that the SCP technique improves the BER performance of 2×2 MIMO self-het OFDM with Alamouti code and Golden code by 3.5dB and 3.3dB at BER of 10^{-3} , respectively. We also showed that the proposed SCP STBC MIMO self-het OFDM outperforms the conventional scheme with superheterodyne receivers at high SNRs in the presence of phase noise. Finally, we conclude that, the phase noise immunity is essential for OFDM systems with small subcarrier spacing, which are heavily degraded by large phase noise found in mm-Wave receivers.

APPENDIX A PROOF OF PROPOSITION 1

Consider a 2×2 MIMO self-het OFDM using an Alamouti code over MIMO fading channels. From the equivalent model in (10), we obtain

$$\begin{aligned} \mathbf{H}_{\text{eq}}^H \hat{\mathbf{Y}} &= \mathbf{H}_{\text{eq}}^H \mathbf{H}_{\text{eq}} \mathbf{S} + \mathbf{H}_{\text{eq}}^H \hat{\mathbf{Z}} \\ &= \Lambda \mathbf{S} + \mathbf{H}_{\text{eq}}^H \hat{\mathbf{Z}} \end{aligned} \quad (18)$$

where Λ is given in (12). Let $\tilde{\mathbf{Z}} \triangleq \mathbf{H}_{\text{eq}}^H \hat{\mathbf{Z}} = [\tilde{Z}_1, \tilde{Z}_2]^T$ and $\mathbf{S} = [S_1, S_2]^T$. Without loss of generality, the instantaneous SINR γ associated with S_1 , from (18), is given by

$$\begin{aligned} \gamma &= \frac{|\Lambda S_1|^2}{E \left(|\tilde{Z}_1|^2 \right)} = \Lambda \frac{E_s}{\sigma_{\tilde{Z}_1}^2} \\ &= \Lambda \bar{\gamma} \end{aligned} \quad (19)$$

where $\sigma_{\tilde{Z}_1}^2$ is given by (8) and $\bar{\gamma} = E_s/\sigma_{\tilde{Z}_1}^2$ is the average SINR in the k -th OFDM subcarrier. For QPSK signalling, the error probability at the k -th OFDM subcarrier is given by

$$P_e(k) = \int_0^\infty Q(\sqrt{x\bar{\gamma}}) f_\Lambda(x) dx. \quad (20)$$

Since there is no simple analytical expression for $f_\Lambda(x)$, it is difficult to determine (20). In order to evaluate the asymptotic behavior of $P_e(k)$, we use the fact that the diversity order of a fading channel is determined by the behavior of $f_\Lambda(x)$ around zero [33]. This is equivalent to the asymptotic behavior of the Laplace transform of $f_\Lambda(x)$ at infinity [33], i.e., if

$$\lim_{s \rightarrow \infty} \mathcal{L}(f_\Lambda) = bs^{-d} + O(s^{-(d+\epsilon)}), \quad (21)$$

then the diversity order is d for some positive constants b and ϵ .

Let $\nu_1 \triangleq \sum_{m=1}^2 |H_{1m}|^2$, $\nu_2 \triangleq \sum_{m=1}^2 |H_{2m}|^2$, $\hat{\alpha} \triangleq |\alpha_c|^2$ and $\hat{\beta} \triangleq |\beta_c|^2$. Since α_c and β_c are complex Gaussian random variables, both $\hat{\alpha}$ and $\hat{\beta}$ follow an exponential distribution,

i.e. $\sim \exp(1/2)$. Since $|H_{rm}|^2 \sim \exp(1)$, then $\nu_1, \nu_2 \sim \text{Erlang}(2, 1)$. The random variables ν_1 and $\hat{\alpha}$ are independent since the RF carrier and the k -th OFDM subcarrier are separated by a minimum of B_g . The cdf of Λ_1 in (12) then can be written as

$$\begin{aligned} F_{\Lambda_1}(x) &= \int_0^\infty \int_0^{\hat{\alpha}} \frac{\nu_1}{2} \exp(-\nu_1) \exp\left(-\frac{1}{2}\hat{\alpha}\right) d\nu_1 d\hat{\alpha} \\ &= 1 - xK_2(\sqrt{2x}) \end{aligned} \quad (22)$$

where $K_v(\cdot)$ denotes the v -th order of modified Bessel function of second kind. Then, the pdf of x can be written as

$$\begin{aligned} f_{\Lambda_1}(x) &= \frac{d}{dx} F_{\Lambda_1}(x) \\ &= -K_2(\sqrt{2x}) + \frac{\sqrt{2x}}{4} \left(K_1(\sqrt{2x}) + K_3(\sqrt{2x}) \right). \end{aligned} \quad (23)$$

Using the recursive property of the modified Bessel functions (i.e. $zK_{v-1}(z) - zK_{v+1}(z) = -2vK_v(z)$) [34], $f_{\Lambda_1}(x)$ can be further simplified to

$$f_{\Lambda_1}(x) = \frac{\sqrt{2x}}{2} K_1(\sqrt{2x}). \quad (24)$$

The Laplace Transform of $f_{\Lambda_1}(x)$ is given by

$$\mathcal{L}(f_{\Lambda_1})(s) = \frac{2s + e^{\frac{1}{2s}} \mathbb{Ei}\left(-\frac{1}{2s}\right)}{4s^2} \quad (25)$$

where $\mathbb{Ei}(\cdot)$ is the exponential integral and it is defined as $\mathbb{Ei}(z) \triangleq -\int_z^\infty \exp(-t)/t dt$. Similar expression to (25) can be derived for $f_{\Lambda_2}(x)$.

Since Λ_1 and Λ_2 are independent, the Laplace transform of the pdf of Λ , $\mathcal{L}(f_\Lambda)(s)$, is given by the product of the individual Laplace transforms, i.e.,

$$\begin{aligned} \mathcal{L}(f_\Lambda)(s) &= f_{\Lambda_1}(s) \times f_{\Lambda_2}(s) \\ &= \frac{1}{4s^2} + \frac{e^{\frac{1}{2s}} \mathbb{Ei}\left(-\frac{1}{2s}\right)}{4s^3} + \frac{e^{\frac{1}{s}} \mathbb{Ei}\left(-\frac{1}{s}\right)^2}{16s^4} \\ &= \frac{1}{4} s^{-2} + O\left(s^{-(2+\epsilon^+)}\right). \end{aligned} \quad (26)$$

Using the property in (21), we find that the diversity order is 2. ■

APPENDIX B PROOF OF PROPOSITION 2

Considering an Alamouti code is used in this system, we maximize the received RF carrier power at a single receive antenna, i.e., maximizing $|\alpha_c|^2$ only. Then, the RF carrier is positioned such that $l^* = \arg \max_{l \in 1, N} \left\{ |\alpha_c^{(l)}|^2 \right\}$ and l^* is the new RF carrier location. This gives the lower bound of the achievable diversity improvement using the SCP technique.

Let $\hat{\alpha}_1 \triangleq |\alpha_c^{(1)}|^2$, $\hat{\alpha}_N \triangleq |\alpha_c^{(N)}|^2$, $\hat{\alpha} \triangleq |\alpha_c^{(l^*)}|^2$, and $\nu_1 \triangleq \sum_{m=1}^2 |H_{1m}^{(k)}|^2$. Since the first and the N -th OFDM subcarriers are located apart, it is reasonable to assume that those channels undergo independent fading. Hence, the cdf of $\hat{\alpha}$ is given as

$$F_{\hat{\alpha}}(x) = F_{\hat{\alpha}_1}(x) \times F_{\hat{\alpha}_N}(x) = \left\{ 1 - e^{(-x/2)} \right\}^2$$

and the pdf is given as

$$f_{\hat{\alpha}}(x) = \frac{d}{dx} \{F_{\hat{\alpha}}(x)\} = e^{(-x/2)} \left\{ 1 - e^{(-x/2)} \right\}.$$

We note that the distribution of ν_1 remains unchanged (i.e. $\nu_1 \sim \text{Erlang}(2, 1)$). Hence, similar to Appendix A, the pdf of Λ_1 is given by

$$f_{\Lambda_1}(x) = \sqrt{2x} K_1(\sqrt{2x}) - 2\sqrt{x} K_1(2\sqrt{x}). \quad (27)$$

and its Laplace transform is given by

$$\mathcal{L}(f_{\Lambda_1})(s) = \frac{e^{\frac{1}{2s}} \mathbb{Ei}\left(-\frac{1}{2s}\right) - 2e^{\frac{1}{s}} \mathbb{Ei}\left(-\frac{1}{s}\right)}{2s^2}. \quad (28)$$

Although the distribution Λ_1 is altered, the distribution of Λ_2 remains unchanged and its Laplace transform can be compute similarly to (25). Then the Laplace transform of $f_\Lambda(x)$ can be written as

$$\begin{aligned} \mathcal{L}(f_\Lambda)(s) &= \frac{e^{\frac{1}{2s}} \mathbb{Ei}\left(-\frac{1}{2s}\right)}{4s^3} - \frac{e^{\frac{1}{s}} \mathbb{Ei}\left(-\frac{1}{s}\right)}{2s^3} \\ &\quad - \frac{e^{\frac{3}{2s}} \mathbb{Ei}\left(-\frac{1}{s}\right) \mathbb{Ei}\left(-\frac{1}{2s}\right)}{4s^4} + \frac{e^{\frac{1}{s}} \mathbb{Ei}\left(-\frac{1}{s}\right)^2}{8s^4} \end{aligned} \quad (29)$$

since Λ_1 and Λ_2 are independent. As $s \rightarrow \infty$, $\mathcal{L}(f_\Lambda)(s)$ can be expanded as

$$\lim_{s \rightarrow \infty} \mathcal{L}(f_\Lambda)(s) = \frac{\zeta + \log\left(\frac{2}{s}\right)}{4s^3} + O\left(s^{-(3+\epsilon)}\right) \quad (30)$$

where ζ is the Euler–Mascheroni constant and $\epsilon > 0$. Using (21), we see that lower bound on the diversity order is 3. ■

APPENDIX C PROOF OF PROPOSITION 3

Using an Alamouti code for enhanced 2×2 MIMO self-het OFDM, we maximize the received RF carrier power for both receive antennas independently, i.e. maximize both $|\alpha_c|^2$ and $|\beta_c|^2$ separately. Since the RF carrier locations at both transmitter antennas should be the same, this maximization is impossible. Instead, we analyze the upper bound of the diversity order using the SCP technique. In this case, the pdfs of both Λ_1 and Λ_2 are given in (27). Hence, the Laplace transform of $f_\Lambda(x)$ for this particular case can be written as

$$\begin{aligned} \mathcal{L}(f_\Lambda)(s) &= f_{\Lambda_1}(s) \times f_{\Lambda_2}(s) \\ &= \frac{\left(e^{\frac{1}{2s}} \mathbb{Ei}\left(-\frac{1}{2s}\right) - 2e^{\frac{1}{s}} \mathbb{Ei}\left(-\frac{1}{s}\right) \right)^2}{4s^4}. \end{aligned} \quad (31)$$

As $s \rightarrow \infty$, $\mathcal{L}(f_\Lambda)(s)$ can be expand as

$$\lim_{s \rightarrow \infty} \mathcal{L}(f_\Lambda)(s) \approx \frac{(\zeta + \log(2))^2}{4s^4} + O\left(s^{-(4+\epsilon^+)}\right). \quad (32)$$

Using (21), the upper bound on the diversity order is 4. ■

ACKNOWLEDGMENT

This work was performed at the Monash Software Defined Telecommunications Lab and supported by the Australian Research Council Discovery project ARC DP130100336.

REFERENCES

- [1] P. Smulders, "Exploiting the 60GHz band for local wireless multimedia access: prospects and future directions," *IEEE Comm. Magazine*, vol. 40, no. 1, pp. 140–147, Jan 2002.
- [2] H.-J. Song and T. Nagatsuma, "Present and future of terahertz communications," *IEEE Trans. on Terahertz Science and Tech.*, vol. 1, no. 1, pp. 256–263, Sept. 2011.
- [3] Y. Shoji, M. Nagatsuka, K. Hamaguchi, and H. Ogawa, "60GHz band 64 QAM/OFDM terrestrial digital broadcasting signal transmission by using millimeter-wave self-heterodyne system," *IEEE Trans. on Broadcasting*, vol. 47, no. 3, pp. 218–227, Sept. 2001.
- [4] T. Nagatsuma, "Generating millimeter and terahertz waves," *IEEE Microwave Magazine*, vol.10, no.4, pp.64,74, June 2009.
- [5] K. Ono, T. Saito, N. Hidaka, Y. Ohashi, ; Y. Aoki, "A 60-GHz HEMT-based MMIC direct-detection receiver for application in non-contact ID card systems," 25th European Microwave Conference, vol.2, no., pp. 996–1000, Sept. 1995
- [6] J.N.Schulman, V. Kolinko, M. Morgan, C. Martin, J. Lovberg, S. Thomas, J. Zinck, Y.K. Boegeman, "W-band direct detection circuit performance with Sb-heterostructure diodes," *IEEE Microwave and Wireless Components Letters*, vol.14, no.7, pp. 316–318, July 2004
- [7] Y. Shoji, K. Hamaguchi, and H. Ogawa, "Millimeter-wave remote self-heterodyne system for extremely stable and low-cost broad-band signal transmission," *IEEE Trans. on Microwave Theory and Tech.*, vol. 50, no. 6, pp. 1458–1468, June 2002.
- [8] Y. Shoji, H. Ogawa, "70-GHz-band MMIC transceiver with integrated antenna diversity system: application of receiver-module-arrayed self-heterodyne technique," *IEEE Transactions on Microwave Theory and Techniques*, vol.52, no.11, pp. 2541–2549, Nov. 2004
- [9] C. Choi and Y. Shoji, "Third-order intermodulation distortion characteristics of millimeter-wave self-heterodyne transmission techniques," in *Asia-Pacific Microwave Conference, 2006. APMC2006*, Dec. 2006, pp. 1751–1756.
- [10] Y. Shoji and H. Ogawa, "High-receiving-sensitivity 70-GHz band MMIC transceiver: application of receiving-module-arrayed self-heterodyne technique," in *IEEE MTT-S International Microwave Symposium Digest, 2004*, vol. 1, June 2004, pp. 219–222.
- [11] C. Choi, Y. Shoji, and H. Ogawa, "Analysis of receiver space diversity gain for millimeter-wave self-heterodyne transmission techniques under two-path channel environments," in *IEEE Radio and Wireless Symposium, 2007*, Jan. 2007, pp. 75–78.
- [12] Y. Shoji, C. Choi, and H. Ogawa, "Millimeter-wave OFDM WPAN system applying adaptive modulation for grouped sub-carriers," in *IEEE Radio and Wireless Symposium, 2007*, Jan. 2007, pp. 499–502.
- [13] C. Choi, Y. Shoji, and H. Ogawa, "Implementation of an OFDM base-band with adaptive modulations to grouped subcarriers for millimeter-wave wireless indoor networks," *IEEE Transactions on Consumer Electronics*, vol. 57, no. 4, pp. 1541–1549, Nov. 2011.
- [14] Y. Haibing, P.F.M. Smulders, and M.H.A.J. Herben, "Frequency Selectivity of 60-GHz LOS and NLOS Indoor Radio Channels," in *IEEE Vehicular Technology Conference, 2006. VTC 2006-Spring*, May. 2006, pp. 2727–2731.
- [15] P. Smulders, "Statistical Characterization of 60-GHz Indoor Radio Channels," *IEEE Transactions on Antennas and Propagation*, vol. 57, no. 10, pp. 2820–2829, Oct. 2009
- [16] X. Hao, V. Kukshya, T.S. Rappaport, "Spatial and temporal characteristics of 60-GHz indoor channels," *IEEE Journal on Selected Areas in Communications*, vol. 20, no. 3, pp.620–630, Apr. 2002.
- [17] Y. Azar, G.N. Wong, T.S. Rappaport, "28 GHz Propagation Measurement or outdoor cellular communication using steerable beam antenna," in *2013 IEEE International Conference on Communications (ICC 13)*, Budapest, Hungary, Jun. 2013.
- [18] N. Fernando, Y. Hong, and E. Viterbo, "Self-heterodyne OFDM transmission for frequency selective channels," *IEEE Trans. on Commun.*, vol. 61, no. 5, pp. 1936–1946, May 2013.
- [19] N. Fernando, Y. Hong, and E. Viterbo, "Subcarrier Pairing for Self-Heterodyne OFDM," in *2013 IEEE International Conference on Communications (ICC 13)*, Budapest, Hungary, Jun. 2013.
- [20] H. Zhang, S. Venkateswaran, U. Madhow, "Channel Modeling and MIMO Capacity for Outdoor Millimeter wave Links," in *IEEE Wireless Communications and Networking Conference*, Sydney, Australia, pp. 1–4, Apr. 2010.
- [21] E. Torkildson, H. Zhang, U. Madhow, "Channel Modeling for Millimeter Wave MIMO," in *Information Theory and Applications Workshop(ITA)*, San Diego, CA, Feb. 2010.
- [22] H. Bolcskei and A. J Paulraj, "Space-frequency coded broadband OFDM systems," in *IEEE Wireless Communications and Networking Conference*, Chicago, IL, USA, pp. 1–6, Sept. 2000.
- [23] S. Alamouti, "A simple transmit diversity technique for wireless communications," *IEEE Journal on Selected Areas in Communications*, vol. 16, no.8, pp. 1451–1458, Oct. 1998. doi:10.1109/49.730453
- [24] P. Xia, S. Zhou, and G.B. Giannakis, "Adaptive MIMO-OFDM based on partial channel state information," *IEEE Transactions on Signal Processing*, vol.52, no.1, pp. 202–213, Jan. 2004
- [25] J.C. Belfiore, G. Rekaya, and E. Viterbo, "The golden code: a 2×2 full-rate space-time code with nonvanishing determinants," *IEEE Transactions on Information Theory*, vol.51, no.4, pp. 1432–1436, April 2005.
- [26] L. Zheng, and D.N.C. Tse, "Diversity and multiplexing: a fundamental tradeoff in multiple-antenna channels," *IEEE Transactions on Information Theory*, vol.49, no.5, pp.1073–1096, May 2003.
- [27] E. Viterbo and J. Boutros, "A universal lattice code decoder for fading channels," *IEEE Transactions on Information Theory*, vol.45, no.5, pp. 1639–1642, Jul. 1999.
- [28] V. Tarokh, N. Seshadri, A.R. Calderbank, "Space-time codes for high data rate wireless communication: Performance criterion and code construction," *IEEE Transactions on Information Theory*, vol. 44, no. 2, pp. 744–765, March 1998.
- [29] O. Tirkkonen and A. Hottinen, "Square-matrix embeddable space-time block codes for complex signal constellations," *IEEE Transactions on Information Theory*, vol.48, no.2, pp. 384–395, Feb. 2002.
- [30] E. Biglieri, Y. Hong, and E. Viterbo, "On Fast-Decodable SpaceTime Block Codes," *IEEE Transactions on Information Theory*, vol.55, no.2, pp. 524–530, Feb. 2009.
- [31] S. Wu and Y. Bar-Ness, "OFDM systems in the presence of phase noise: consequences and solutions," *IEEE Transactions on Communications*, vol. 52, no. 11, pp. 1988–1996, Nov. 2004.
- [32] R.C. Daniels and R.W. Heath, "60GHz wireless communications: emerging requirements and design recommendations," *IEEE Vehicular Technology Magazine*, vol. 2, no. 3, pp. 41–50, Sept. 2007.
- [33] W. Zhengdao and G.B. Giannakis, "A simple and general parameterization quantifying performance in fading channels," *IEEE Transactions on Communications*, vol.51, no.8, pp. 1389–1398, Aug. 2003.
- [34] I. S. Gradshteyn, I.M Ryzhik, A. Jeffrey, and D. Zwillinger, *Table of Integrals, Series, and Products*, 6-th ed, Academic Press, 2000.
- [35] "Wireless LAN at 60 GHz - IEEE 802.11ad Explained", *application note-Agilent technology*, 2013.
- [36] "TGad Evaluation Methodology", *IEEE 802.11-09/0296r16*, 2010.
- [37] S. Skotnikov, "Low Power LDPC Decoder design for 802.11ad standard", Master thesis, 2012.



Nirmal Fernando received the B.Sc (Hones), and PG.Dip degrees from the Department of Electronic and Telecommunication Engineering, University of Moratuwa, Sri Lanka, in 2009 and 2009, respectively. He received his PhD degree from the Department of Electrical and Computer Systems Engineering, Monash University, Australia, in 2014. He is currently working as a Project Technical Leader at Airservices Australia, Brisbane. From 2009 to 2010, he has been working as a lecturer at University of Moratuwa, Sri Lanka, from 2006 to 2009, as an Engineer in Dialog Telekom, Sri Lanka. His research interests include non-coherent OFDM techniques, low complexity RF receivers, Optical OFDM, MIMO precoding, signal processing in wireless communications and communication theory.



Yi Hong (M'00–SM'10) is currently a Senior Lecturer at the Department of Electrical and Computer Systems Eng., at Monash University, Clayton, Australia. She received her Ph.D. degree in Electrical Engineering and Telecommunications from the University of New South Wales (UNSW), Sydney, Australia, in Oct. 2004. She then worked at the Institute of Telecom. Research, University of South Australia, Australia; at the Institute of Advanced Telecom., Swansea University, UK; and at University of Calabria, Italy. During her PhD, she

received an International Postgraduate Research Scholarship (IPRS) from the Commonwealth of Australia; a supplementary Engineering Award from the School of Electrical Engineering and Telecommunications, UNSW; and a Wireless Data Communication System Scholarship from UNSW. She received the NICTA-ACoRN Earlier Career Researcher award for a paper presented at the Australian Communication Theory Workshop (AUSCTW), Adelaide, Australia, 2007. Dr. Hong is an Associate Editor for European Transactions on Telecommunications and an IEEE Senior member. She was the General Co-Chair of 2014 IEEE Information Theory Workshop, Hobart, Tasmania; and the Technical Program Committee Chair of 2011 Australian Communications Theory Workshop, Melbourne, Australia. She was the Publicity Chair at the 2009 IEEE Information Theory Workshop, Sicily, Italy. She is a Technical Program Committee member for many IEEE conferences such as IEEE ICC, VTC, PIMRC and WCNC. Her research interests include information and communication theory with applications to telecommunication engineering.



Emanuele Viterbo (M'95–SM'04–F'11) was born in Torino, Italy, in 1966. He received his degree (Laurea) in Electrical Engineering in 1989 and his Ph.D. in 1995 in Electrical Engineering, both from the Politecnico di Torino, Torino, Italy. From 1990 to 1992 he was with the European Patent Office, The Hague, The Netherlands, as a patent examiner in the field of dynamic recording and error-control coding. Between 1995 and 1997 he held a post-doctoral position in the Dipartimento di Elettronica of the Politecnico di Torino in Communications Techniques over

Fading Channels. He became Associate Professor at Politecnico di Torino, Dipartimento di Elettronica in 2005 and a Full Professor in DEIS at Università della Calabria, Italy, in 2006. Since 2010, he is a Full Professor at Department of Electrical and Computer Systems Engineering, Monash University, and the Associate Dean Research Training of the Faculty of Engineering at Monash. In 1993 he was visiting researcher in the Communications Department of DLR, Oberpfaffenhofen, Germany. In 1994 and 1995 he was visiting the E.N.S.T., Paris. In 1998 he was visiting researcher in the Information Sciences Research Center of AT&T Research, Florham Park, NJ. In 2003 he was visiting researcher at the Maths Department of EPFL, Lausanne, Switzerland. In 2004 he was visiting researcher at the Telecommunications Department of UNICAMP, Campinas, Brazil. In 2005 he was visiting researcher at the ITR of UniSA, Adelaide, Australia. Dr. Emanuele Viterbo was awarded a NATO Advanced Fellowship in 1997 from the Italian National Research Council. His main research interests are in lattice codes for the Gaussian and fading channels, algebraic coding theory, algebraic space-time coding, digital terrestrial television broadcasting, and digital magnetic recording. He was Associate Editor of IEEE Transactions on Information Theory, European Transactions on Telecommunications and Journal of Communications and Networks; and is now an Editor of Foundations and Trends in Communications and Information Theory.